Steric and Electronic Situation in the 4-X-4 ''-[(4 ''-Y-Phenyl)ethynyl])biphenyl Homologous Series: A Joint Theoretical and Spectroscopic Study

ARTICLE *in* THE JOURNAL OF PHYSICAL CHEMISTRY A · MARCH 2010

Impact Factor: 2.69 · DOI: 10.1021/jp911163t · Source: PubMed

Steric and Electronic Situation in the 4-X-4′-[(4″-Y-Phenyl)ethynyl]biphenyl Homologous Series: A Joint Theoretical and Spectroscopic Study

Pedro D. Ortiz,[†,||] Reynier Suardíaz,[‡,§] Laura de Vega,[†] Gunther Hennrich,*[,†] and Pedro J. Ortiz*[,‡]

Departamento de Química Orgánica y Departamento de Química-Física Aplicada, Universidad Autónoma de Madrid, Madrid, 28049, Spain, and Departamento de Química-Física, Universidad de La Habana, La Habana 10400, Cuba

Received: November 24, 2009; Revised Manuscript Received: January 5, 2010

In this work we have studied the rotational barriers, the polarization of the acetylenic triple bond, and the molecular dipole moments in the 4-X-4′-[(4″-Y-phenyl)ethynyl]biphenyl homologous series using the density functional theory (DFT) and 1D/2D NMR spectroscopy. This series of compounds constitutes an effective base for the acquisition of liquid crystals. The equilibrium angle (θ_{eq}) and the torsional barriers $\Delta E(0°)$ and $\Delta E(90°)$ are not very sensitive to the substituent effects. We have found evidence for the similarity in the π-conjugation of the Y-substituted and X,Y-disubstituted compounds, the latter with mesomorphic properties, by means of the graphic analysis of the relationship between the molecular dipolar moment μ(D) and the difference between the ^{13}C NMR chemical shifts of the acetylenic carbon atoms ($\Delta\delta_{CI\equiv CII}$ [ppm]). The obtained results contribute to a better understanding of the structure−activity relationship for potential liquid crystalline systems.

1. Introduction

Liquid crystals are substances that show anisotropic properties as solids, combined with a degree of fluidity characteristic of liquids.[1,2] For this singular behavior, liquid crystals are of great importance for high quality displays and other modern device manufacture.[3−7]

Thermal and dynamic properties of mesogenic compounds are strongly influenced by both electronic and molecular structure of individual building units, as well as the intermolecular interactions operative in the bulk.[8−11] The mesomorphic behavior of an organic compound can be varied by modifying its molecular structure.[12] For example, the molecular order in the liquid crystal phase depends on the mesogenic core structure and its geometry, polarizability, molecular conformation, and permanent dipole moment.

In this work we have studied molecules of the 4-X-4′-[(4″-Y-phenyl)ethynyl]biphenyl homologous series, with the biphenyl fragment being a common structural motif for thermotropic calamitic liquid crystals[13] (Scheme 1).

It is important to obtain information about the effect of the terminal substituents (X, Y) on the biphenyl fragment and the carbon−carbon triple bond. For biphenyl systems, Johansson and Olsen reported values very close to the experimentally obtained equilibrium angle and torsion barriers using a combination of coupled cluster, density functional theory, and thermal corrections.[14−16]

In order to obtain geometrical and spectroscopic data, keeping the computational effort within reasonable limits, we explore the possibility whether useful results can be achieved using the density functional theory (DFT) approach as a theoretical method. DFT calculations have proved to be an accurate method for the evaluation of different properties for a plethora of molecular systems including biphenyl systems.[14,17,18]

SCHEME 1: Molecular Structure of 4-X-4′-[(4′-Y-Phenyl)etheny]biphenyl

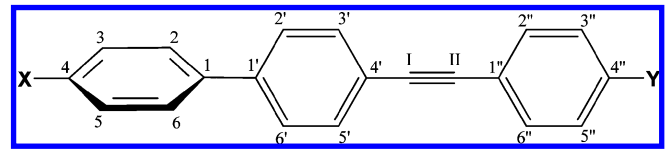

2. Methods

2.1. Theoretical Calculations. The geometry optimizations and the calculation of frequencies were performed at the DFT[19,20] level using the B3LYP functional and 6-311G(d,p) basis set.[21,22]

The ^{13}C NMR nuclear chemical shielding tensors were calculated by the gauge-including atomic orbital (GIAO) method.[23,24] In our case, it can be assumed that the length of side chains does not play a significant role in the electronic properties of the target molecules. Therefore, all alkyl side chains have been replaced by CH_3 groups in the corresponding theoretical models, in order to reduce calculation complexity.

For comparison with experimental NMR data, the δ(ppm) relative chemical shifts were calculated by referring the absolute shielding tensor obtained by DFT to the absolute shielding tensor of tetramethylsilane (TMS), 184.5 ppm, which was calculated at the same level of theory. The value of σ_{iso} for TMS obtained by us is very close to that obtained after correction by vibrational averaging, for bulk susceptibility, for temperature, and in relation to a secondary standard, 185.4 ppm.[25] These results confirm the appropriateness of the basis set and functional used in our chemical shifts calculation. All quantum chemical calculations are performed using the Gaussian 03 program package.[26]

* Authors to whom correspondence should be addressed. (P.J.O.) E-mail: pedro@fq.uh.cu; (G.H.) E-mail: gunther.hennrich@uam.es.
† Departamento de Química Orgánica, Universidad Autónoma de Madrid.
‡ Universidad de La Habana.
§ Departamento de Química-Física Aplicada, Universidad Autónoma de Madrid.
|| Present address: Departamento de Química Inorgánica, Universidad de La Habana, La Habana 10400, Cuba.

10.1021/jp911163t
Published on Web 02/01/2010

SCHEME 2: Molecular Structure of Biphenyl

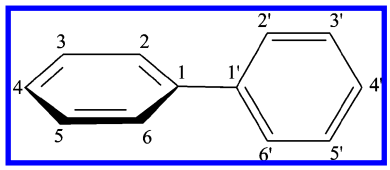

TABLE 1: Calculated and Experimental Torsional Barriers and Equilibrium Angle of Biphenyl

	ΔE (0°) (kJ/mol)	ΔE (90°) (kJ/mol)	θ° (equilibrium)
experimental	6.0 ± 2.1[15]	6.5 ± 2.1[15]	44.4 ± 1.2[16]
calculated[14]	8.0	8.3	39.5
calculated[a]	9.0	8.3	40.6

[a] This work.

TABLE 2: Experimental and Calculated ^{13}C NMR Chemical Shifts Differences between the Acetylenic Carbon Atoms ($\Delta\delta_{CI\equiv CII}$ (ppm) = $\delta_{CI} - \delta_{CII}$)

molecule			
X	Y	$\Delta\delta_{CI\equiv CII}$(ppm) calculated	$\Delta\delta_{CI\equiv CII}$(ppm) experimental
$OC_{10}H_{21}$	Pyr	+7.2	+7.4[28]
$OC_{10}H_{21}$	NO_2	+9.1	+6.9[28]
$OC_{10}H_{21}$	$COOCH_3$	+4.3	+3.3[28]
$COOCH_3$	$OC_{10}H_{21}$	−3.9	−3.2[28]
$COCH_3$	NH_2	−5.6	−6.3[29]

2.2. ^{13}C NMR Spectra. NMR spectra were recorded at 300 K in partially deuterated chloroform (deuteration grade 99.80%) on a Bruker AC 300 spectrometer (75 MHz for ^{13}C), and the chemical shits, δ(ppm), were referenced to the residual $CDCl_3$ signal. The g-HMBC (gradient-heteronuclear multiple bond correlation) was recorded at 300 K using a Varian NMR System 400 (100 MHz for ^{13}C).

3. Validation of the Theoretical Level Used in the Present Work

3.1. Torsional Barriers and Equilibrium Angle. The twisted structure of the biphenyl fragment is explained by the balance between ortho hydrogen−hydrogen steric repulsion and the electronic conjugation of the two phenyl rings[27] (Scheme 2).

Table 1 shows that the values for the torsional barriers in the biphenyl fragment obtained in the present work are in good agreement with both experimental data and data obtained using a very high level of theory.[14]The experimental equilibrium angle is larger that the theoretical one obtained at zero temperature, but it is in good agreement with most related methods.[14] Thermal corrections have a large effects on the equilibrium angle because potential energy near the minimum is very shallow, however, for our calculus these corrections are irrelevant.

3.2. ^{13}C NMR Chemical Shifts: Experimental and DFT-GIAO Calculation. Table 2 shows a good agreement between the experimental and theoretical values of the chemical shifts differences between the acetylenic carbon atoms.

The ^{13}C NMR chemical shift DFT-GIAO calculation shows that $\delta_{CI} > \delta_{CII}$ when Y = electron-withdrawing group and $\delta_{CI} < \delta_{CII}$ when Y = electron-donating group, in correspondence with a Hammett plot (Figure 1).

The values of $\Delta\delta$(ppm) = $\delta_{CI} - \delta_{CII}$ contain useful information on the molecular structure of these compounds because they are related with the polarization of the acetylenic triple bond.[30−32] The increased polarization of this bond enhances the cumulenic character and therefore increases efficient π-conjugation (Scheme 3).

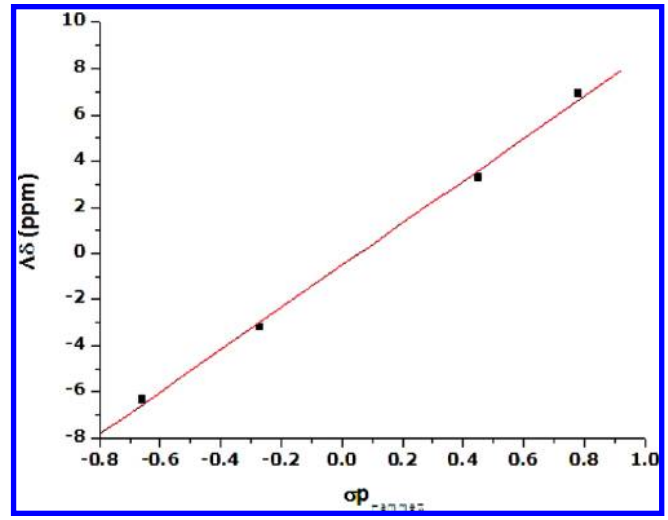

Figure 1. Experimental ^{13}C NMR chemical shifts, $\Delta\delta_{CI\equiv CII}$ (ppm) vs $\sigma p_{Hammett}$ plot.

SCHEME 3: Charge Effect on CI Acetylenic Carbon Atom: Y-Electron-Withdrawing (A) or Y-Electron-Donating (B) Substituent

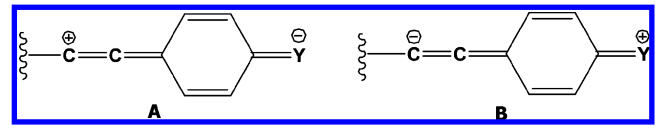

An important result of our analysis is the unequivocal assignment of the C_I and C_{II} chemical shifts in the ^{13}C NMR spectra. Figure 2 shows the g-HMBC spectra of the compound $COCH_3/NH_2$ (a) and $OC_{10}H_{21}/NO_2$ (b), respectively. This 2D NMR technique detects heteronuclear conectivities through two and three bonds, and it is very useful for the identification of quaternary carbon atoms. For simplicity, ^{13}C NMR spectra are not shown in Figure 1 (ppm).

In accordance with the numeration of the atoms, see Scheme 1, three bonds exist from $H_{3'}$ to C_I, as well as from $H_{2''}$ to C_{II}. We will use the proton spectrum-like reference to determine the relative positions of C_I and C_{II} in the ^{13}C NMR spectrum through the cross-peaks of the g-HMBC spectrum.

In the region corresponding to aromatic protons of both molecules the signals corresponding to three different spin systems are observed. The signals of $H_{3'}$ and $H_{2'}$ protons are easily identifiable in both proton spectra. The signals of C_I and C_{II} atoms are in the region of 80−100 ppm of the ^{13}C NMR spectra.

The cross-peaks in Figure 2a show that for the compound $COCH_3/NH_2$ the carbon atom C_I is more shielded than C_{II}, while in Figure 2b it is observed that for the $OC_{10}H_{21}/NO_2$ compound, the carbon atom C_I is more deshielded than C_{II}. Thus, by means of the g-HMBC spectra, a totally sure determination of the acetylenic carbon atom relative position in the ^{13}C NMR spectra is achieved for the studied series of compounds. Those relative positions vary as a function of the electronic characteristic of the Y substituent.

It is important to highlight that by means of the GIAO−DFT method we arrived to the same conclusion in our work. It is firm evidence of the predictive capacity of this theoretical method, at the level we have used it, to predict NMR chemical shifts in the series of studied compounds. The NMR/DFT combination has been also successfully employed in other molecular systems.[33−36]

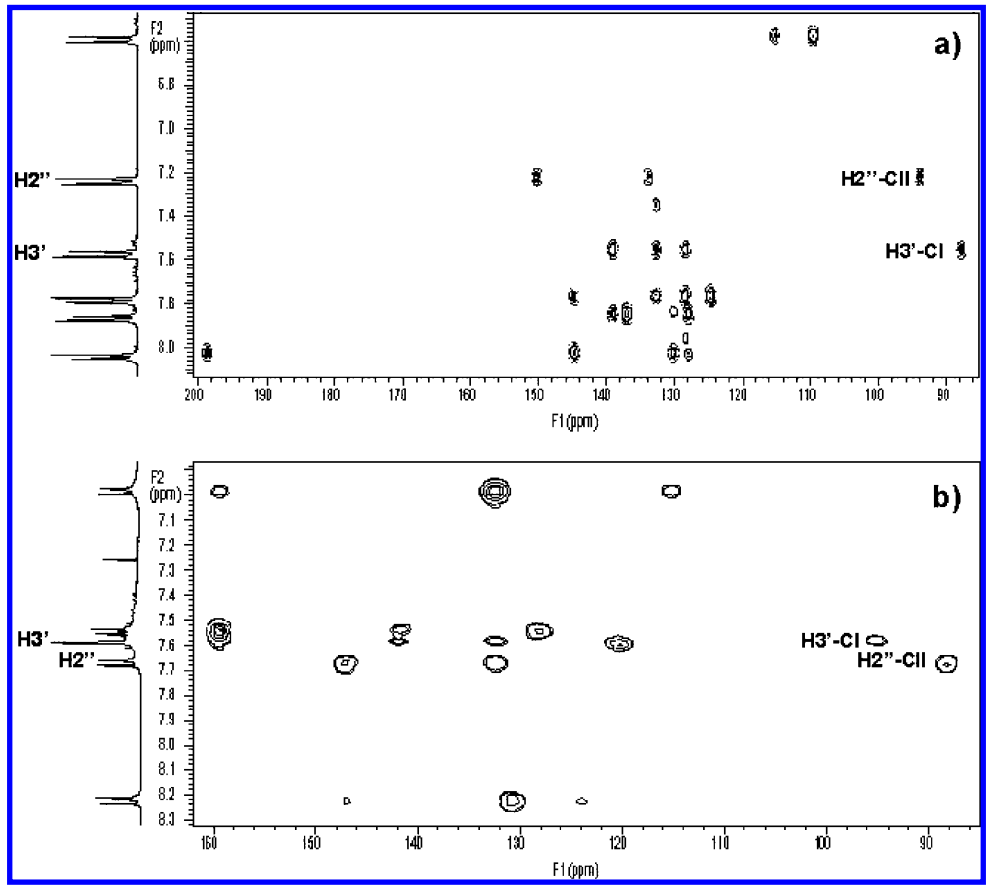

Figure 2. g-HMBC spectra of (a) X = $COCH_3$/Y = NH_2 and (b) X = $OC_{10}H_{21}$/Y = NO_2.

TABLE 3: Calculated Energetic, Geometric, and Spectroscopic Parameters for a Substituent

molecule						
X	Y	θ_{eq}	E_{eq}(a.u.)	bar 0° (kJ/mol)	bar 90° (kJ/mol)	$\Delta\delta_{CI\equiv CII}$ (ppm)
H	H	38.7	−770.70329	8.02	9.20	−0.5
H	NO_2	38.5	−975.25956	8.04	9.30	+8.0
H	$COOCH_3$	38.6	−998.64509	8.04	9.21	+3.2
H	OCH_3	38.5	−885.25746	7.99	9.25	−2.6
H	NH_2	38.5	−826.07788	7.95	9.34	−4.4
NO_2	H	37.6	−975.25983	7.46	10.37	−4.1
$COOCH_3$	H	37.8	−998.64523	7.55	10.13	−2.2
OCH_3	H	37.4	−885.25698	7.20	10.12	−0.1
NH_2	H	36.3	−826.07701	6.62	10.98	+0.6

TABLE 4: Calculated Critical Interatomic Distances for θ = 0°, θ_{eq}, and 90° of the Monosubstituted Compounds

molecule						
X	Y	$d_{C1-C1'}$ (θ_{eq}) (Å)	$d_{C1-C1'}$ (0°) (Å)	$d_{C1-C1'}$ (90°) (Å)	$d_{H2-H2'}$ (θ_{eq}) (Å)	$d_{H2-H2'}$ (0°) (Å)
H	H	1.494	1.494	1.495	2.371	1.950
H	NO_2	1.493	1.490	1.494	2.369	1.951
H	$COOCH_3$	1.493	1.490	1.494	2.371	1.951
H	OCH_3	1.493	1.490	1.494	2.371	1.953
H	NH_2	1.493	1.494	1.494	2.371	1.954
NO_2	H	1.491	1.487	1.493	2.352	1.949
$COOCH_3$	H	1.482	1.488	1.493	2.357	1.952
OCH_3	H	1.491	1.487	1.494	2.359	1.962
NH_2	H	1.490	1.490	1.494	2.342	1.954

4. Torsional Barriers, Equilibrium Angle, and $\Delta\delta_{CI\equiv CII}$ (ppm) of 4-X-4′-[(4-Y-Phenyl)]ethenyl]biphenyl Series

4.1. The Effect of a Substituent. Table 3 summarizes the theoretical values of X- or Y-substituted biphenylacetylene systems. For comparison, the values obtained for X = Y = H are added. The changes in θ_{eq} upon Y-substitution are negligible, but a slight decrease upon the X-substitution can be observed. The biggest effect corresponds to X = NH_2, which is a strong electron-donor substituent.

As can be observed in Table 3, the electronic energy is practically insensitive to the substituent change, and the numeric values indicate that these are stable molecules in all cases. A considerable influence on the torsional barriers is observed for X-substituents. $\Delta E(0°)$ decreases and $\Delta E(90°)$ increases with respect to X = H, and the highest effect is observed when X = NH_2. This result is in agreement with that obtained for the equilibrium angle θ_{eq}, and it is a consequence of the variation of the electron density in the corresponding phenyl ring. The decrease of θ_{eq} results in a stronger repulsion of the hydrogen atoms in the ortho positions of both phenyl rings and therefore an increase in the energy barrier $\Delta E(90°)$. The effect for the Y-substituent is insignificant.

On the other hand, the effect of the Y-substituent on $\Delta\delta_{CI\equiv CII}$ (ppm) is very significant and shows a behavior similar to that described in Section 3.2, with the biggest calculated value of $\Delta\delta_{CI\equiv CII}$ (ppm) for Y = NO_2. The effect is small for the electron-donor substituents OCH_3 and NH_2 but remarkable for the NO_2 group.

It is interesting to observe the relative positions of the acetylenic carbon atoms in the ^{13}C NMR spectrum when one electron-withdrawing substituent occupies the X or Y positions. C_I is the more deshielded nucleus when X = NO_2 and C_{II} is the more deshielded nucleus when Y = NO_2.

The energetics of the internal rotation around the central C−C bond in the biphenyl moiety has proven to be problematic.[37] Although a commonly accepted interpretation exists,[27] a different approach outlines that the hydrogen−hydrogen interaction would in fact be attractive and that the reason for nonplanarity instead

TABLE 5: Calculated Energetic, Geometric and Spectroscopic Parameters for Two Substituents

molecule								
X	Y	θ_{eq}	E_{eq}(a. u.)	bar 0° (kJ/mol)	bar 90° (kJ/mol)	$d_{C1-C1'}$(Å)	$d_{H2-H2'}$(Å)	$\Delta\delta_{CI\equiv CII}$(ppm)
H	H	38.7	−770.70329	8.02	9.20	1.494	2.371	−0.5
$COOCH_3$	NO_2	38.0	−1203.20111	7.65	9.91	1.493	2.357	+7.2
$COCH_3$	NO_2	37.8	−1127.94671	7.48	9.95	1.494	2.342	+7.0
OCH_3	NO_2	36.8	−1089.81355	6.94	10.28	1.494	2.359	+9.1
OCH_3	$COOCH_3$	37.2	−1113.19890	7.09	10.32	1.493	2.352	+4.3
OCH_3	Pyr	37.2	−901.29520	7.11	10.37	1.494	2.369	+7.2
$COOCH_3$	OCH_3	37.5	−1113.19954	7.40	10.28	1.494	2.371	−3.9
$COCH_3$	NH_2	37.1	−978.76583	7.11	10.62	1.494	2.371	−5.6

is caused by an unfavorable lengthening of the central C−C bond when the two benzene rings become more coplanar.[38]

In order to understand the nature of phenyl−phenyl interactions, in Table 4 we summarize the effect of the X- or Y-substituents on critical interatomic distances for the dihedral angle θ equal to 0°, θ_{eq}, and 90°. As can be seen in the table, the bond length of bridging C−C bond, $d_{C1-C1'}$, does not change upon substitution for all dihedral angles.

It is noticeable that $d_{C1-C1'}$ is almost the value of a single bond distance. At the same time, $d_{C1-C1'}$ (θ_{eq}) ≈ $d_{C1-C1'}$ (0°) and $d_{H2-H2'}$ (θ_{eq}) > $d_{H2-H2'}$ (0°) for each molecule. These results support the classical interpretation of the twisted structure of the biphenyl unit.

The calculation method used by us predicts that the X-substituent has the most marked effect on both θ_{eq} and the torsional barriers $\Delta E(0°)$ and $\Delta E(90°)$, while the difference between the chemical shifts of the C_I and C_{II} carbon atoms are more sensitive to the Y-substituent. It also correctly predicts the substitution effect on the geometric and electronic situation, which varies depending on the electronic nature of the substituent.

4.2. The Effect of Two Substituents. Table 5 shows the calculations for X-Y combinations of practical interest in the context of liquid crystals. Obtaining information on the geometric, energetic, and electronic parameters of this series of compounds is especially important.

The effect of X,Y-disubstitution on electronic energy is similar to that observed in monosubstitution. In accordance with the analysis carried out in Section 4.1, we interpret the values of θ_{eq}, $\Delta E(0°)$, $\Delta E(90°)$, $d_{C1-C1'}$, and $d_{H2-H2'}$ in terms of the Y-substituent effects on the X-substituted compounds, and the $\Delta\delta_{CI\equiv CII}$ (ppm) values due to variation of the X-substituent in the Y-substituted compounds. For calculated combinations of X and Y, the following results are obtained, in all cases referenced to the nonsubstituted compound (X = Y = H): θ_{eq} shows little variation, while the torsional barriers $\Delta E(0°)$ and $\Delta E(90°)$ are smaller and bigger, respectively, when they are compared with those of X = Y = H. These results indicate that X-Y double substitution lightly favors the minor θ_{eq} in all cases.

On the other hand, the values of $d_{C1-C1'}$ and $d_{H2-H2'}$ are practically insensitive to the double substitution, as well as in the case of the monosubstitution. Furthermore, $d_{C1-C1'}(\theta_{eq})$ ≈ $d_{C1-C1'}(0°)$ and $d_{H2-H2'}(\theta_{eq}) > d_{H2-H2'}(0°)$, supporting the classical interpretation of the twisted biphenylic structure.

The other important calculated parameter is $\Delta\delta_{CI\equiv CII}$ (ppm). Molecules with Y= NO_2 show the highest values of $\Delta\delta_{CI\equiv CII}$ (ppm), with the highest value for the combination OCH_3/NO_2. The relative position of the C_I and C_{II} carbon atoms in the ^{13}C NMR spectra is in accordance with that obtained for the monosubstituted compounds.

TABLE 6: Calculated Electronic Dipolar Moments, μ(D), for Mono- and Disubstituted Molecules

molecule			molecule		
X	Y	μ (D)	X	Y	μ (D)
H	H	0.17	H	H	0.17
H	NO_2	6.61	$COOCH_3$	NO_2	5.49
H	$COOCH_3$	2.43	$COCH_3$	NO_2	4.49
H	OCH_3	1.84	OCH_3	NO_2	8.07
H	NH_2	2.84	OCH_3	$COOCH_3$	3.21
NO_2	H	5.96	OCH_3	Pyr	4.98
$COOCH_3$	H	2.10	$COOCH_3$	OCH_3	3.01
OCH_3	H	1.80	$COCH_3$	NH_2	5.95
NH_2	H	2.79			

5. Molecular Dipole Moment

Since practical applications of liquid crystals are based on the response of those substances to external electric fields, we will pay special attention to the calculation of the molecular dipole moment.

5.1. Calculated Dipole Moments. In Table 6 it can be seen that all substituted compounds obviously have a higher dipolar moment compared to the unsubstituted reference. The μ(D) value for one substituent is slightly higher when it occupies the Y-position than when it occupies the X-position in the molecule. In the series of monosubstitued compounds, the biggest effect in μ(D) corresponds to the NO_2 group, that takes a significantly high value compared to those calculated for the rest of substituents.

Table 6 shows that the substituent combinations electron-donating (B)/electron-withdrawing (A) lead to an increase of μ(D) increment regarding the monosubstitued compounds, while the substituent combinations A/B give a relative decreases of μ(D). The highest value in the whole series of compounds is found for OCH_3/NO_2 (μ = 8.07 D). In this case there are two substituents with complementary electronic effects.

5.2. Relationship between μ(D) and $|\Delta\delta_{CI\equiv CII}$ (ppm)|. With the objective of obtaining information on the relationship between μ(D) and the acetylenic triple bond polarization, figure 3 shows the μ(D) vs $|\Delta\delta_{CI\equiv CII}$(ppm)| plot for monosubstituted compounds. A linear relationship exists for Y-substituents (Figure 3b), that we interpret in terms of the polarization of the triple bond induced by the Y. The great dispersion of data points observed for the X-substitution (Figure 3a) is evidence of a more complicated relationship between the molecular structure and the electronic conjugation in the π-system.

We have drawn a similar plot (Figure 4), choosing four disubstituted compounds, for which the liquid crystalline properties of their corresponding experimental homologous have been proven experimentally.[28] Figure 4 shows an equally linear relationship as the one observed for Y-substituted compounds (Figure 3b). This is an evidence of the similarity between the

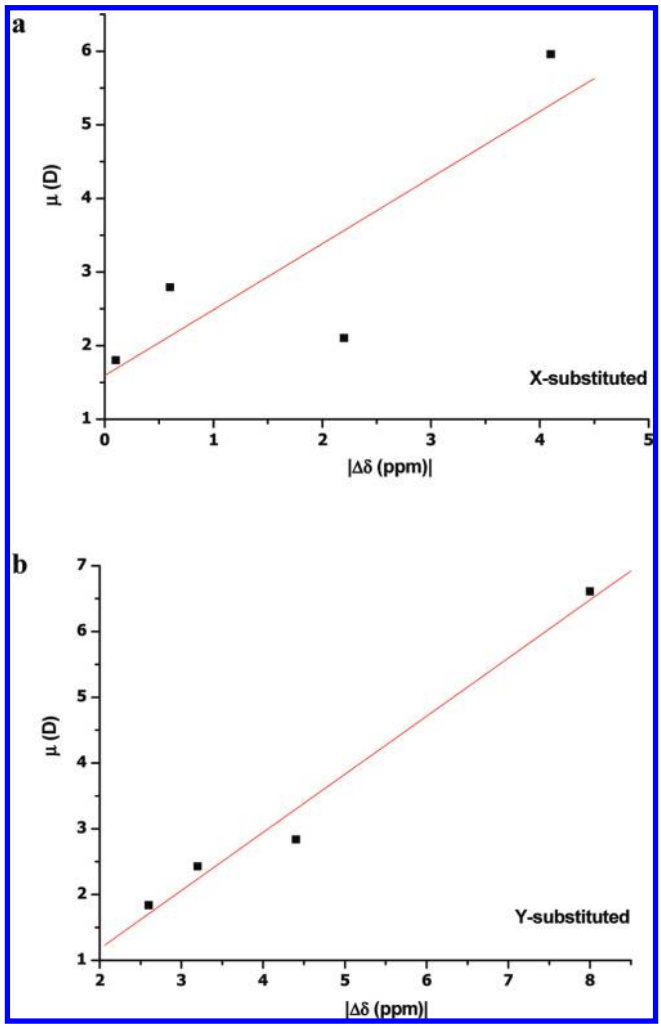

Figure 3. Theoretical μ(D) vs $|\Delta\delta_{CI\equiv CII}$ (ppm)| plot of (a) X- and (b) Y-monosubstituted compounds.

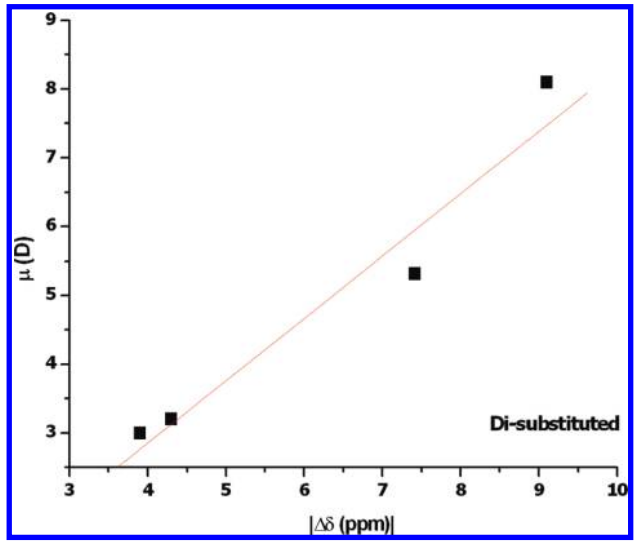

Figure 4. Theoretical μ(D) vs $|\Delta\delta_{CI\equiv CII}$ (ppm)| plot of disubstituted compounds which display liquid crystal properties.

electronic transmission mechanisms in these molecules, and about the contribution of the acetylenic triple bond to this mechanism.

6. Conclusions

In this work we have been able to obtain and to systematize valuable information on the 4-X-4′-[(4-Y-phenyl)ethynyl]biphenyl homologous series of compounds by means of the DFT theory using the B3LYP functional and 6-311G(d,p) bases of functions. ^{13}C NMR chemical shifts calculations carried out by means of the GIAO method, at the same theory level, are equally satisfactory. The equilibrium angle (θ_{eq}) is in the range of 38.5−36.3°, and the method of calculus also predicts correctly the $\Delta E(0°)$ and $\Delta E(90°)$ torsional barriers, in good agreement with that obtained by means of others theoretical and experimental methods for the biphenyl and its para,para′-disubstituted derivatives. In the series that we study, these parameters are dependent on the X-substitution. In general, those molecules of the series that have substituents with high electronic effects, i.e., the combinations electron-donating/electron-withdrawing and electron-withdrawing/electron-donating, are effective to obtain high electric dipolar moment μ(D) values. It is a very important parameter because of its relationship with the liquid crystal properties of these compounds. The functional relationship between μ(D) and $|\Delta\delta_{CI\equiv CII}$(ppm)| is similar for both Y- and disubstituted molecules (the latter with properties like those of liquid crystals).

Acknowledgment. The financial support by the UAM/CCC and the MEC (project CTQ2007-65683) is gratefully acknowledged.

References and Notes

(1) Lagerwaall, J. P. F.; Giesselmam, F. *ChemPhysChem.* **2006**, *7*, 20–45.
(2) Burnell, E. E.; de Lange, C. A. *Chem. Rev.* **1998**, *98*, 2359–2387.
(3) Kim, J. B.; Choi, C. J.; Park, J. S.; Jo, S. J.; Hwang, B. H.; Jo, M. K.; Kang, D.; Lee, S. J.; Kim, Y. S.; Baik, H. K. *Adv. Mater.* **2008**, *20*, 3073–3078.
(4) Vaughn, K. E.; Sousa, M.; Kang, D.; Rosenblett, C. *Appl. Phys. Lett.* **2007**, *90*, 194102/1–194102/3.
(5) Yi, Y.; Nakata, M.; Martín, A. R.; Clark, N. A. *Appl. Phys. Lett.* **2007**, *90*, 63510/1–163510/3.
(6) Gu, M.; Smalysukh, I. I.; Lavrentovich, O. D. *Appl. Phys. Lett.* **2006**, *88*, 061110/1−061110/3.
(7) Kohki, T.; Maski, H.; Mitsuhiro, K.; Nobuyuki, I.; Ray, H.; Masanori, S. Alignment *Technologies and Applications of Liquids Crystals Devices*; Taylor & Francis: New York, 2005.
(8) Modliska, A.; Inglot, K.; Martyski, T.; Dbrowski, R.; Jofyn, J.; Baumam, D. *Liq. Cryst.* **2009**, *36* (2), 197–208.
(9) Kang, H.; Sohn, E. H.; Kand, D.; Lee, J. Ch. *Liq. Cryst.* **2009**, *36* (8), 855–864.
(10) Ree, M. *Macromol. Res.* **2006**, *14*, 1–33.
(11) Ichimura, K. *Chem. Rev.* **2000**, *100*, 1847–1874.
(12) Ha, S. T.; Koh, T. M.; Liu, H. C.; Yeap, G. Y.; Win, Y. F.; Ong, S. T.; Sivasothy, Y.; Ong, L. K. *Liq. Cryst.* **2009**, *36* (9), 917–925.
(13) Hennrich, G.; Ortiz, P. D.; Cavero, E.; Hanes, R. E.; Serrano, J. L. *Eur. J. Org. Chem.* **2008**, 4575–4579.
(14) Johanson, M. P.; Olsen, J. J. *Chem. Theory. Comput.* **2008**, *4*, 1460–1471.
(15) Bastiansen, O.; Samdal, S. *J. Mol. Struct.* **1985**, *128*, 115–125.
(16) Almenningen, A.; Bastiansen, O.; Fernholt, L.; Cyvin, B. N.; Cyvin, S. J.; Samdal, S. *J. Mol. Struct.* **1985**, *128*, 59–76.
(17) Kaupp, M.; Buhl, M.; Malkin, B. G. *Calculation of NMR and EPR Parameters*; Wiley VCH: Weinheim, Germany, 2004.
(18) Vaara, J. *Phys. Chem. Chem. Phys.* **2007**, *9*, 5399–5418.
(19) Hohenberg, P.; Kohn, W. *Phys. Rev.* **1964**, *136*, B864–B871.
(20) Kohn, W.; Sham, L. J. *Phys. Rev.* **1965**, *140*, A1133–A1138.
(21) Becke, A. D. *J. Chem. Phys.* **1993**, *98*, 5648–5652.
(22) Lee, C.; Yang, W.; Parr, R. G. *Phys. Rev. B* **1988**, *37*, 785–789.
(23) Wolinshi, K.; Hilto, J. F.; Pulay, P. J. *J. Am. Chem. Soc.* **1990**, *112*, 8251–8260.
(24) Ditchfield, R. *Mol. Phys.* **1974**, *27*, 789–796.
(25) Mason, J. *Multinuclear NMR*; Plenum Press: New York, 1987; Ch. 3.
(26) Frisch, M. J.; Trucks, G. W.; Schlegel, H. B.; Scuseria, G. E.; Robb, M. A.; Cheeseman, J. R.; Montgomery J. A., Jr.; Vreven, T.; Kudin, K. N.; Burant, J. C.; Millam, J. M.; Iyengar, S. S.; Tomasi, J.; Barone, V.; Mennucci, B.; Cossi, M.; Scalmani, G.; Rega, N.; Petersson, G. A.; Nakatsuji, H.; Hada, M.; Ehara, M.; Toyota, K.; Fukuda, R.; Hasegawa, J.; Ishida, M.; Nakajima, T.; Honda, Y.; Kitao, O.; Nakai, H.; Klene, M.; Li, X.; Knox, J. E.; Hratchian, H. P.; Cross, J. B.; Bakken, V.; Adamo, C.; Jaramillo, J.; Gomperts, R.; Stratmann, R. E.; Yazyev, O.; Austin, A. J.; Cammi, R.; Pomelli, C.; Ochterski, J. W.; Ayala, P. Y.; Morokuma, K.; Voth, G. A.; Salvador, P.; Dannenberg, J. J.; Zakrzewski, V. G.; Dapprich, S.; Daniels, A. D.; Strain, M. C.; Farkas, O.; Malick, D. K.; Rabuck, A. D.;

Raghavachari, K.; Foresman, J. B.; Ortiz, J. V.; Cui, Q.; Baboul, A. G.; Clifford, S.; Cioslowski, J.; Stefanov, B. B.; Liu, G.; Liashenko, A.; Piskorz, P.; Komaromi, I.; Martin, R. L.; Fox, D. J.; Keith, T.; Al.Laham, M. A.; Peng, C. Y.; Nanayakkara, A.; Challacombe, M.; Gill, P. M. W.; Johnson, B.; Chen, W.; Wong, M. W.; Gonzalez, C.; Pople, J. A. Gaussian 03, Gaussian, Inc., Wallingford, CT, 2004.

(27) Poater, J.; Solá, M.; Bickelhautpt, F. *Chem.—Eur. J.* **2006**, *12*, 2889–2895.

(28) De Vega, L.; Ortiz, P. D.; Hennrich, G.; Omenat, A.; Tejedor, R. M.; Barbera, J.; Gomez-Lor, B.; Serrano, J. L. *J. Phys. Chem. B* submitted.

(29) 4-Ethanone-yl-4′-[(4″-aminophenyl)ethynyl]biphenyl (X = $COCH_3$/Y = NH_2) as a yellow solid. Yield: 95 mg; 31%; ^{1}H NMR: δ = 8.04 ppm (d, J = 8.1 Hz, 2 H); 7.85 (d, J = 8.1, 2 H); 7.77 (d, J = 8.2, 2 H); 7.56 (d, J = 8.2, 2 H); 7.24 (d, J = 8.0, 2 H); 6.60 (d, 2 H); 2.60 (s, 3 H). ^{13}C NMR: δ = 198.1 ppm; 149.8, 144.0, 138.0, 136.2, 133.6, 132.0, 129.6, 127.8, 127.4, 123.9, 113.9, 109.2, 93.2, 86.9, 26.8; MALDI-HRMS found: 311.3879; calculated for $C_{22}H_7ON$: 311.3869. R_f (Hex/EtOAc 1:1): 0.28.

(30) Keinpeter, E.; Schielenberg, A. *J. Org. Chem.* **2006**, *71*, 3869.

(31) Meier, H.; Mühling, B.; Oehlhof, A.; Theisinger, S.; Kristen, E. *Eur. J. Org. Chem.* **2006**, 405.

(32) Rubin, M.; Trofimov, V.; Gevorgyan, V. *J. Am. Chem. Soc.* **2005**, *127*, 10243.

(33) Platts, J. A.; Gkionis, K. *Phys. Chem. Chem. Phys.* **2009**, *11*, 10331.

(34) Bifulco, G.; Dambruoso, P.; Gomez-Paloma, L.; Riccio, R. *Chem. Rev.* **2007**, *107*, 3744.

(35) d'Antuono, P.; Botek, E.; Champagne, B.; Wieme, J.; Reyniers, M.-F.; Marin, G. B. *J. Phys. Chem. B* **2008**, *112*, 14804.

(36) Wittala, K. W.; Hoye, T. R.; Cramer, C. J. *J. Chem. Theory Comput.* **2006**, *2*, 1085.

(37) Pacios, L. F. *Struct. Chem.* **2007**, *18*, 785.

(38) Matta, C.; Hernández-Trujillo, J.; Tang, T.-H.; Bader, R. F. W. *Chem.—Eur. J.* **2003**, *9*, 1940.

JP911163T